CellPress

Cell Stem Cell
Article

Myelodysplastic Cells in Patients Reprogram Mesenchymal Stromal Cells to Establish a Transplantable Stem Cell Niche Disease Unit

Hind Medyouf,[1,11,13,*] Maximilian Mossner,[2] Johann-Christoph Jann,[2] Florian Nolte,[2] Simon Raffel,[3] Carl Herrmann,[4,5] Amelie Lier,[3] Christian Eisen,[3] Verena Nowak,[2] Bettina Zens,[1,3] Katja Müdder,[1,3] Corinna Klein,[1,3] Julia Obländer,[2] Stephanie Fey,[2] Jovita Vogler,[2] Alice Fabarius,[2] Eva Riedl,[6] Henning Roehl,[7] Alexander Kohlmann,[8] Marita Staller,[8] Claudia Haferlach,[8] Nadine Müller,[2] Thilo John,[9] Uwe Platzbecker,[10] Georgia Metzgeroth,[2] Wolf-Karsten Hofmann,[2] Andreas Trumpp,[1,3,11,12,*] and Daniel Nowak[2,12]

[1]Division of Stem Cells and Cancer, Deutsches Krebsforschungszentrum (DKFZ), Im Neuenheimer Feld 280, 69120 Heidelberg, Germany
[2]Department of Hematology and Oncology, University Hospital Mannheim, Medical Faculty Mannheim of the University of Heidelberg, 68167 Mannheim, Germany
[3]Heidelberg Institute for Stem Cell Technology and Experimental Medicine (HI-STEM gGmbH), Im Neuenheimer Feld 280, 69120 Heidelberg, German
[4]Institute of Pharmacy and Molecular Biotechnology, University of Heidelberg, 69120 Heidelberg, Germany
[5]Division of Theoretical Bioinformatics, DKFZ, 69120 Heidelberg, Germany
[6]Department of Pathology, University Hospital Mannheim, 68167 Mannheim, Germany
[7]Department of Orthopedics, University Hospital Mannheim, 68167 Mannheim, Germany
[8]Munich Leukemia Laboratory (MLL), 81377 Munich, Germany
[9]Department of Traumatology, DRK Hospital Westend, 14050 Berlin, Germany
[10]Technical University Dresden, University Hospital 'Carl Gustav Carus,' Medical Clinic and Policlinic I, 01307 Dresden, Germany
[11]German Cancer Consortium, 69120 Heidelberg, Germany
[12]These authors contributed equally to this work and are co-senior authors
[13]Present address: Technical University Dresden, University Hospital 'Carl Gustav Carus,' Medical Clinic and Policlinic I, 01307 Dresden, Germany
*Correspondence: hind.medyouf@uniklinikum-dresden.de (H.M.), a.trumpp@dkfz-heidelberg.de or andreas.trumpp@hi-stem.de (A.T.)
http://dx.doi.org/10.1016/j.stem.2014.02.014

SUMMARY

Myelodysplastic syndromes (MDSs) are a heterogeneous group of myeloid neoplasms with defects in hematopoietic stem and progenitor cells (HSPCs) and possibly the HSPC niche. Here, we show that patient-derived mesenchymal stromal cells (MDS MSCs) display a disturbed differentiation program and are essential for the propagation of MDS-initiating $Lin^{-}CD34^{+}CD38^{-}$ stem cells in orthotopic xenografts. Overproduction of niche factors such as CDH2 (N-Cadherin), IGFBP2, VEGFA, and LIF is associated with the ability of MDS MSCs to enhance MDS expansion. These factors represent putative therapeutic targets in order to disrupt critical hematopoietic-stromal interactions in MDS. Finally, healthy MSCs adopt MDS MSC-like molecular features when exposed to hematopoietic MDS cells, indicative of an instructive remodeling of the microenvironment. Therefore, this patient-derived xenograft model provides functional and molecular evidence that MDS is a complex disease that involves both the hematopoietic and stromal compartments. The resulting deregulated expression of niche factors may well also be a feature of other hematopoietic malignancies.

INTRODUCTION

Myelodysplastic syndromes (MDSs) are a heterogeneous group of malignant clonal diseases that affect older individuals (median age 68–75 years) with an incidence in the range of 3–10/100,000. MDSs are characterized by ineffective hematopoiesis and the presence of dysplastic cells in the bone marrow as well as peripheral cytopenias. Clinically, patients present with symptoms such as anemia, bleeding, or infection. Classification of MDS is carried out according to risk-score systems such as the World Health Organization (WHO) classification or the international prognostic scoring systems (IPSS and IPSS-R). These scoring systems allow the accurate segregation of patients according to prognosis and are used to adapt therapeutic options to individual patients (Garcia-Manero, 2012). Treatment options for MDS range from best supportive care, hematopoietic growth factors, or immunomodulatory drugs such as lenalidomide in lower-risk patients to treatment with DNA demethylating agents, cytotoxic chemotherapy, or hematopoietic stem cell (HSC) transplantation with curative intent for patients in higher-risk subgroups (Garcia-Manero, 2012). Genome-wide discovery approaches recently revealed a number of genetic lesions in patients with MDS that provide valuable insights into the underlying biology of MDS (Haferlach et al., 2014; Bejar et al., 2011, 2012; Papaemmanuil et al., 2013; Walter et al., 2012). This knowledge has been successfully used to generate genetic mouse models of MDS (Abdel-Wahab et al., 2013; Muto et al., 2013). However, it is expected

that no single model can recapitulate the disease heterogeneity and complexity seen in patients.

Several attempts to generate a robust xenograft model in immunodeficient mice have been undertaken, but these have demonstrated inconsistent, transient, and low levels of engraftment, particularly with regard to samples taken from lower-risk MDS patients (Martin et al., 2010; Muguruma et al., 2011; Thanopoulou et al., 2004). In addition, distinguishing normal HSC from MDS stem cell (MDS HSC) engraftment was difficult, given that large cytogenetic lesions that allow easy tracking of the malignant clone are only present in about half of the MDS patients and that no distinguishing cell-surface markers have been identified to date (Martin et al., 2010; Muguruma et al., 2011; Thanopoulou et al., 2004). Most importantly, patient samples that did engraft in these studies represented higher-risk MDS, which are closer to acute myeloid leukemia (AML) (Pang et al., 2013). Recently, several studies suggested that alterations in the bone marrow niche influence the development of myeloid neoplasms (reviewed by Raaijmakers, 2012). Mice deficient for retinoic acid receptor γ (*RARγ*) develop myeloproliferative syndromes induced solely by the RARγ-deficient microenvironment (Walkley et al., 2007). More recently, MDS could efficiently be induced in mice in which *DICER*, a gene encoding a microRNA processing enzyme, was deleted in osteoprogenitor cells (Raaijmakers et al., 2010), whereas expression of an activated form of β-catenin in osteoblasts alters the differentiation of hematopoietic progenitors, leading to the development of AML (Kode et al., 2014). Finally, in chronic myeloid leukemia (CML), niche cells have been shown to exert a protective role in the response to Imatinib in vitro (Zhang et al., 2013). Altogether, these reports strongly support the hypothesis that abnormal niche environment provides ''fertile soil'' for the expansion of the neoplastic cells in vivo.

RESULTS

Cotransplantation of CD34$^+$ Cells with Patient-Derived MSCs Allows Efficient and Long-Term MDS Reinstallment in NSG Mice

Our study is based on the analysis of 31 MDS patients who were classified as follows: IPSS low risk (n = 7), intermediate-1 risk (n = 24), and WHO 2008 classifications MDS 5q (n = 7), MDS RCMD (n = 14), MDS RAEB I (n = 6), MDS-U (n = 2), and MDS RARS (n = 2; Table S1). Among these, 24 were tested for their ability to propagate MDS in a xenograft setting (low risk, n = 5; intermediate-1 risk, n = 19). Based on the hypothesis that disease-propagating cells (DPCs) in lower-risk MDS form a functional unit with their stromal niche cells, we decided to compare the engraftment of MDS-derived CD34$^+$ cells injected either alone or in combination with their corresponding in vitro expanded mesenchymal stromal cells into the bone marrow cavity of sublethally irradiated NOD/LtSz-scid IL2Rγc$^{-/-}$ (NSG) mice (Figure 1A). We opted for the intrabone injection because of the hypothesis that hematopoietic and stromal cells may require physical interaction. Then, mice were analyzed for human chimerism (human CD45 [hCD45] expression) at 16–28 weeks post-transplantation. Of the cases transplanted with CD34$^+$ cells alone, only one of seven samples (MDS14) showed engraftment above the 1% threshold we set for this study (one of three mice engrafted; Figure 1B, left). In contrast, coinjection of CD34$^+$ cells with MDS MSCs resulted in a significantly higher engraftment in 70% of the patient samples analyzed (14 of 20 patients; range = 1%–22%; p = 0.026; Figure 1B). A direct comparison with the identical CD34$^+$ MDS samples was possible for four patients: MDS14, MDS17, MDS18, and MDS19 (Figure 1B). MDS17 did not engraft in either condition. Importantly, the remaining three samples showed an enhanced engraftment with MDS MSCs, further validating our finding.

Abnormal Lineage Distribution and Clonal Tracking of MDS Cells in the Xenograft

Bone marrow cells from engrafted mice were further analyzed with lineage-specific antibodies (CD19 for B cells and CD33 for myeloid cells). When compared to mice repopulated with age-matched healthy old CD34$^+$ cells, most recipients of MDS cells had a significant disproportionate output of myeloid cells (MDS, 70.3% ± 5.3%; healthy, 10.7% ± 1.4%; p < 0.0001; Figure 1C). Four patients (MDS12, MDS24, MDS38, and MDS52) showed an increased B lymphoid output, which may indicate the engraftment of healthy stem cells as opposed to an MDS-derived clone (Figure 1C). To ascertain the origin of the xenografted cells (MDS or healthy), we used several methods to molecularly track the lesions that were initially identified in the patients. Primary hematopoietic cells from each patient were analyzed with chromosomal banding and SNP array (SNP-A) as well as targeted next-generation sequencing (NGS), interrogating acquired mutations in 17 frequently mutated genes described in MDS (Table S2). This strategy allowed us to identify at least one traceable lesion for all patients included in this study with the exception of MDS19 (Table S1). Therefore, bone marrow from patient 19 was subjected to whole-exome sequencing, which revealed the presence of a *BCORL1* mutation in 58% of the bone marrow cells (corresponding to a mutational allele frequency of 29%). Importantly this mutation was not detected in MSCs isolated from the same patient, thereby excluding a germline origin (data not shown). For each engrafted mouse, hCD45$^+$ cells were purified by fluorescence-activated cell sorting (FACS) and analyzed with SNP-A or interphase fluorescence in situ hybridization (FISH) analysis for the detection and quantification of del(5q) or del(21q) (Figures 1D–1F and Table S3) as well as by employing specific pyrosequencing assays in order to track and quantify the mutated alleles (Figure 1G). Table S3 provides a comprehensive summary of the mutational allele frequencies detected in human cells isolated from all xenografted mice displayed in Figure 1B. In the case of cytogenetic aberrations, the numbers refer to the percentage of analyzed cells that scored positive for the lesion, whereas, for heterozygous point mutations, these numbers refer to the allele frequency of the mutated variant. These data confirm that these cells carried the same lesion(s) as the one(s) identified in the original patient samples. Furthermore, we could even observe a significant expansion of an MDS clone carrying both an *SF3B1* mutation and a del(5q) in the mouse engrafted with patient MDS11 cells (Figures 1D and 1E). Even though human cells isolated from MDS16 did not carry any lesion, they exhibited the typical marked myeloid bias observed in most other MDS samples that were validated by molecular analysis (Figure 1C). The predominant B cell population isolated from xenografts of patients

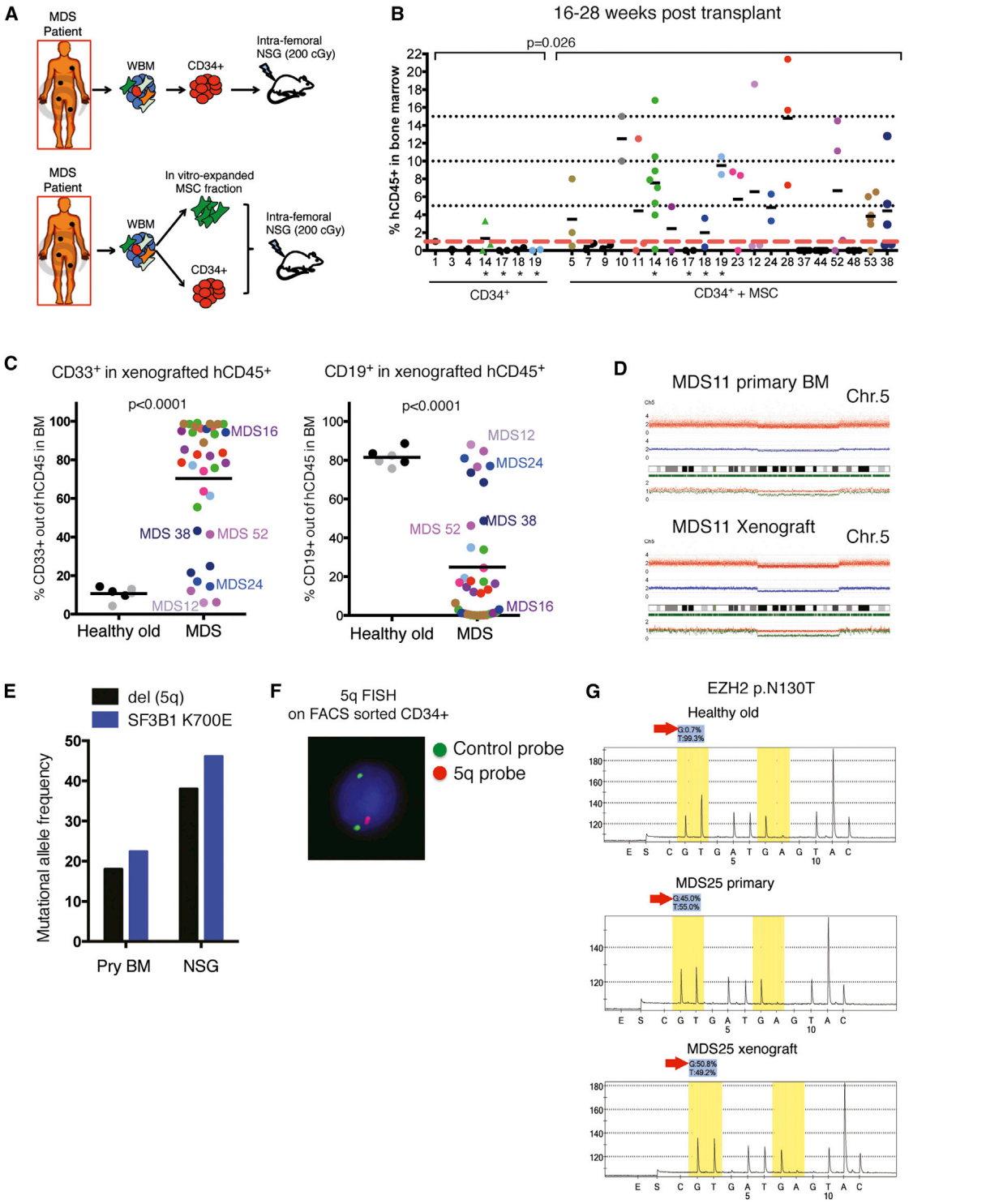

Figure 1. Enhanced Engraftment of Lower-Risk MDS by Cotransplantation of Patient-Derived MSCs

(A) Schematic experimental setup. MDS CD34$^+$ were injected in the bone marrow cavity of sublethally irradiated NSG mice either alone (CD34$^+$) or in combination with MDS-derived MSCs (CD34$^+$ + MSC).

(B) Percentage of hCD45$^+$ cells in the bone marrow of xenografted mice (%hCD45$^+$) analyzed 16–28 weeks posttransplantation. The red dotted line indicates the 1% threshold used in this study to define positive engraftment. Numbers on the x axis are patient IDs. Each dot represents one mouse. Mean engraftment values were compared in the two cohorts with a Mann-Whitney test (p = 0.026). Asterisks indicate paired patient samples analyzed side by side.

(legend continued on next page)

MDS12 and 24 did not carry the mutations present in the patient; however, the CD33$^+$ fraction did (Table S3), indicating the coengraftment of a healthy and an MDS stem cell. Patient 38 engrafted three mice, one of which showed a significant MDS engraftment, whereas the two others mostly gave rise to a B lymphoid-biased graft with cells that did not carry the lesion seen in the original patient.

Human MDS-Initiating Cells display Long-Term Self-Renewal Activity in Serial Transplantation Assays

As expected, human cells with stem cell (CD34$^+$CD38$^-$) and progenitor (CD34$^+$CD38$^+$) phenotypes were detectable in all xenografts with MDS MSCs, albeit at varying frequencies (Figure 2A and data not shown). In addition, analysis of myeloid, and in some cases B lymphoid, cells isolated from NSG xenografts showed that they carried the molecular lesion found in the primary patient (Figures 2B and 2C and data not shown). Because cells with a hematopoietic stem and progenitor cell (HSPC) phenotype were readily detectable in primary xenografts, we addressed whether they could be serially transplanted into secondary recipients. Cells with an hCD45$^+$CD34$^+$ phenotype were isolated with FACS from a mouse previously engrafted with CD34$^+$ cells of patient MDS14 (Figure 2D). The presence of the chromosome 5q deletion was quantified by FISH analysis of FACS-purified human cells (Figure 2E). Then, 10 weeks post-transplantation, two of three recipients engrafted with as little as 6,500 transplanted CD45$^+$CD34$^+$ cells along with MDS MSCs (Figure 2F). Even though the contribution was below 1%, these cells were positive for del(5q), demonstrating their origin from MDS14 (Figure 2E). Similar results were obtained with serial transplantation of CD45$^+$ or CD45$^+$CD34$^+$ cells from patients 10 and 23, respectively (Figure S1A). These data demonstrate that lower-risk MDS stem cells can harbor long-term self-renewal activity.

Higher MDS Engraftment and Typical Signs of Dysplasia in NSGS Recipients

In vitro studies suggest that MSCs and growth factors have synergistic effects on the expansion of HSPCs (Walenda et al., 2011). However, it is well known that a subset of murine growth factors exhibit limited cross-reactivity with the human orthologs of their receptors, which could limit the growth of human stem cells in a murine host (Wunderlich et al., 2010). Therefore, we attempted to further improve human MDS engraftment by using the recently described NSGS mouse strain that constitutively expresses the human cytokines IL3, GM-CSF, and stem cell factor (SCF). These mice have been shown to improve the engraftment of primary human AML (Wunderlich et al., 2010). More recently, investigators demonstrated enhanced normal human myelopoiesis after injection of CD34$^+$ human cord blood cells in this strain (Miller et al., 2013). We compared the engraftment of four patient samples side by side in age-matched NSG and NSGS mice also coinjected with MDS MSCs. This analysis revealed an augmented human chimerism in NSGS in comparison to NSG mice (Figure 3A), which increases over time in the NSGS mice, as indicated by an illustrative example (Figure S1B). Similar to the NSG model, characteristic molecular lesions present in the samples from the patients were also found in the xenografted cells (Figures S1C–S1G). These data are summarized in Figure 3A, in which the mean frequency of MDS cells (hCD45$^+$ cells carrying an MDS lesion) in the bone marrow of NSG or NSGS mice are displayed. These results show a consistently enhanced MDS disease burden in the NSGS strain.

Given that the presence of dysplastic cells is one of the main clinical features of MDS, we performed Pappenheim staining of bone marrow smears in order to analyze the morphology of engrafted cells. This analysis revealed readily detectable dysplastic cells exclusively in mice engrafted with MDS-derived cells (Figure 3B). As shown in Figure 3B, typical signs of dysplastic erythropoiesis with megaloblastic and vacuolized proerythroblasts in both the primary patient bone marrow sample (top right) and the corresponding xenograft (Figure 3B, bottom right) is apparent. Importantly, these dysplastic signs were absent in unmanipulated NSGS mice (Figure 3B, top left) as well as mice engrafted with healthy age-matched CD34$^+$ cells (Figure 3B, bottom left). Altogether, these data indicate that expression of human cytokines further improves the engraftment and growth of human MDS cells in mice.

MDS Initiating and Propagating Cells Have a Lin$^-$CD34$^+$CD38$^-$ Phenotype, Retain Multipotency, and Display Variegated Clonality

The identification of the DPC in human MDS has so far been hampered by the lack of a transplantation assay for this disease. Molecular alterations described in MDS are rarely found in lymphoid compartments, raising the possibility that the MDS-DPC might be a myeloid restricted progenitor rather than an early stem cell harboring both myeloid and lymphoid potential. Alternatively, genetic and/or epigenetic changes in MDS stem cells might prevent their ability to commit to the lymphoid lineage. To address this issue, erythroid (CD235a$^+$ CD71$^+$), myeloid (CD33$^+$), and lymphoid (CD3$^+$CD19$^+$) cells from five primary samples from MDS patients were isolated

(C) Immunophenotyping of hCD45$^+$ cells isolated from the bone marrow of mice engrafted with either MDS (n = 12 patients displayed in B and transplanted in a total of 33 mice) or healthy age-matched CD34$^+$ cells (n = 2 healthy donors each transplanted in three mice) both injected with MDS MSCs. MDS xenografts showed a significant skewing toward myeloid output (unpaired Student's t test, $p < 0.0001$).
(D) High-density SNP array analysis. The shown profile depicts a heterozygous deletion of chromosome 5q in patient MDS11 bone marrow (top) and its corresponding xenograft (bottom).
(E) Molecular analysis of MDS11 primary patient sample (Pry BM) and its corresponding xenograft in an NSG mouse (NSG). Data show the presence of a *SF3B1* mutation (allelic frequency = 22%) and a deletion of chromosome 5q (35% of cells positive; i.e., 17.5% relative allelic frequency displayed in the graph) in the primary patient sample. In the xenograft, MDS cells carrying these lesions expand to allelic frequencies of >40% for *SF3B1* and >35% for del(5q).
(F) Interphase FISH for tracking the chromosome 5q deletion on FACS-sorted human CD34$^+$ cells from a mouse engrafted with patient sample MDS14 cells.
(G) Example of a quantitative pyrosequencing assay designed to track and quantify mutations in primary samples as well as xenografted fractions. The burden of the mutated allele is indicated with a red arrow. Bone marrow from healthy old donors (>60 years) was used as a control.
See also Tables S1, S2, and S3.

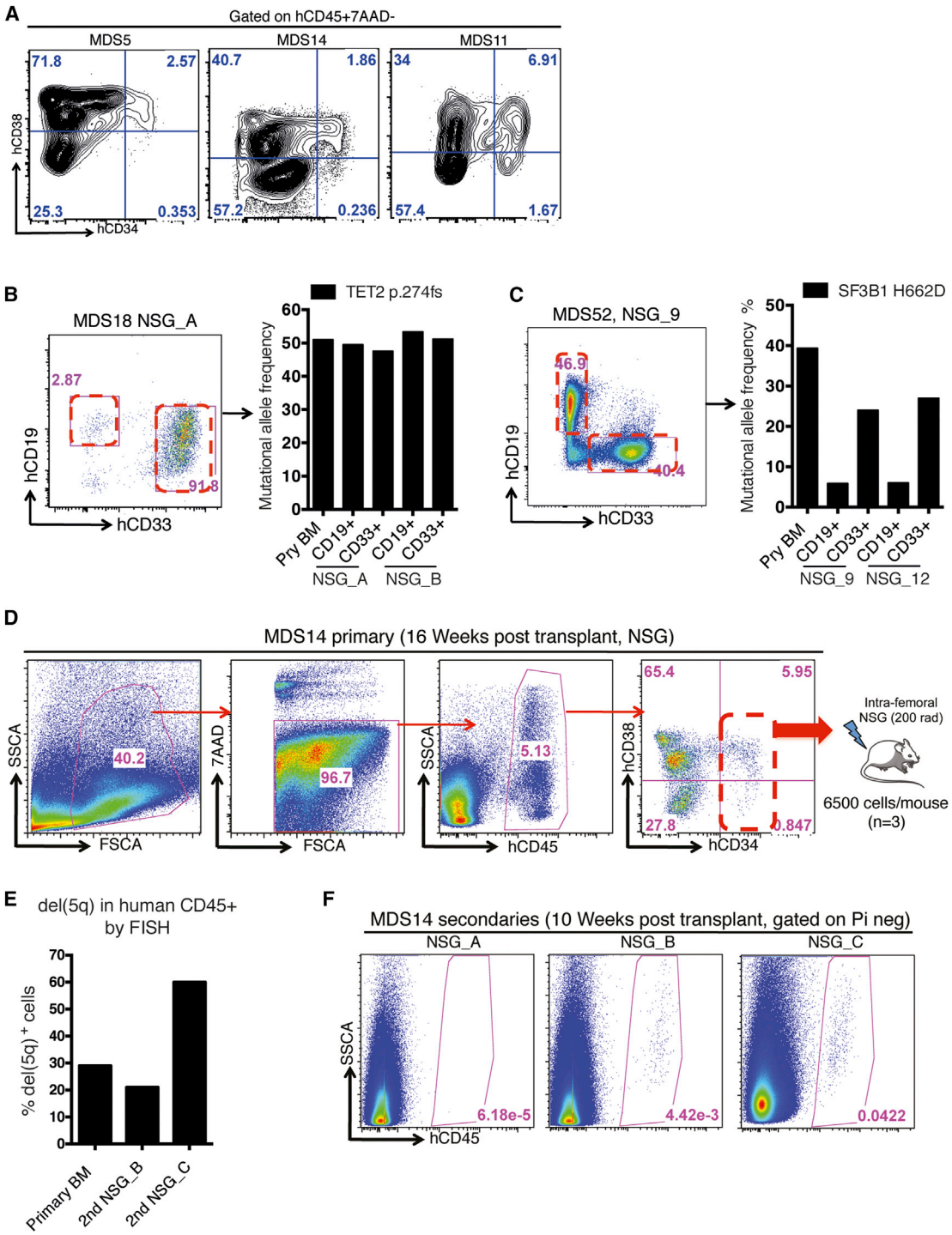

Figure 2. MDS Cells Sustain Long-Term Multilineage Hematopoiesis in NSG Mice

(A) Representative FACS plots showing that human cells with progenitor ($CD34^+CD38^+$) and stem cell ($CD34^+CD38^-$) phenotypes are readily detectable in the xenografts with MDS MSCs 16–28 weeks posttransplantation.

(B) The indicated fractions were purified by FACS and subjected to mutational allele frequency quantification by pyrosequencing.

(B and C) Gating scheme used to sort B lymphoid ($CD19^+$) and myeloid cells ($CD33^+$) form the bone marrow of mice engrafted with cells from patients MDS18 and MDS52.

(D) Workflow of serially transplanting a primary xenografted sample from MDS14 into three secondary recipients 16 weeks after the initial transplant.

(E and F) Secondary xenografts, which were generated by transplanting as little as 6,500 $CD34^+$ cells from the primary mouse retain the primary del(5q) molecular lesion as detected by FISH analysis of FACS-sorted fractions depicted in (F). In all FACS experiments, dead cells were excluded with 7AAD.

See also Figure S1.

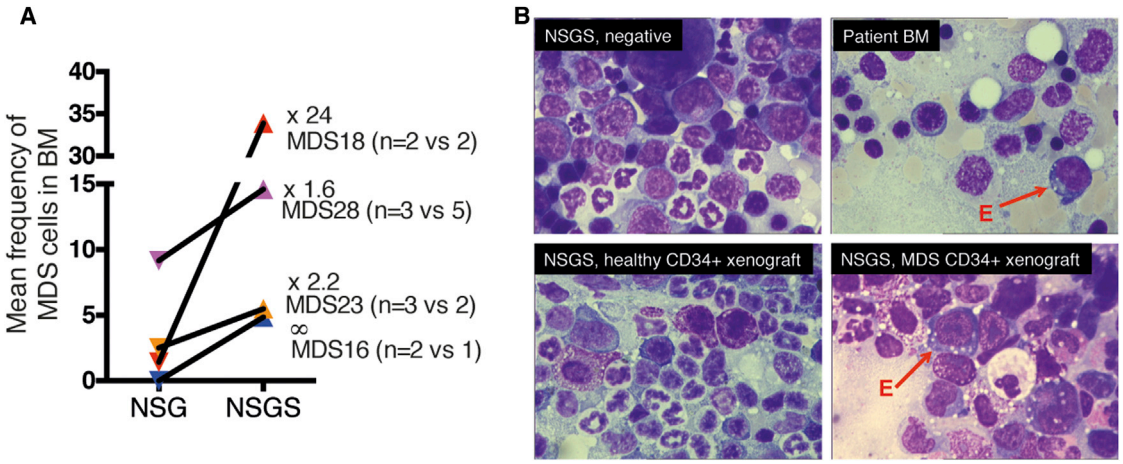

Figure 3. NSGS Mice Further Enhance the Engraftment of Dysplastic MDS Cells

(A) Side by side comparison of engraftment levels in NSG and NSGS mice injected with $CD34^+$ + MDS MSCs derived from four patients (MDS16, MDS18, MDS23, and MDS28). Data show the mean frequency of MDS cells as determined by multiplication of the fraction of $hCD45^+$ cells carrying the MDS-specific molecular lesion by the percentage of $hCD45^+$ cells in the bone marrow of engrafted mice.

(B) Representative example of a Pappenheim staining of bone marrow smears of an untreated native NSGS mouse (upper left), primary MDS patient bone marrow (upper right), NSGS mouse xenotransplanted with $CD34^+$ cells from a healthy donor (lower left), and NSGS mouse xenotransplanted with $CD34^+$ cells from the corresponding MDS patient (lower right). The primary patient bone marrow showed pronounced signs of dysplasia most predominant in the erythropoietic compartment with megaloblastic and vacuolized proerythroblasts (red arrows with "E"). These can also be readily detected in the xenografted NSGS mice from this patient (lower right, red arrow with "E").

See also Figures S1B–S1G and Table S3.

and analyzed for the presence of mutations. These data show that myeloid and erythroid cells are consistently derived from the MDS cells (Figures S2A–S2E). Interestingly, contribution to the lymphoid lineage could also be readily detected in two of the five patients (MDS25 and MDS16). To experimentally identify the stem cell origin of the DPC in lower-risk MDS, we FACS purified stem and progenitor populations of two patients on the basis of lineage negativity (CD235a, CD19, CD4, CD8, and CD20), CD45 positivity, and CD34 and CD38 expression and tested their ability to propagate the MDS cells in NSGS mice (Figure 4A). Each of the four FACS-sorted populations were injected into two or four mice (depending on the number of primary cells recovered) and analyzed after 14–16 weeks posttransplantation for human cell chimerism. As outlined in Figure 4B, engraftment was achieved exclusively in mice that had received the $Lin^-CD34^+CD38^-$ stem cell fraction but not any other cell population. Mutational tracking confirmed the patient origin of the engrafted MDS cells (Figures 4C and 4D).

Analysis of primary bone marrow cells isolated from patient 18 revealed the presence of three mutations (*TET2*, *U2AF1*, and del(*RUNX1*)) that we could track with our established workflow in both NSG and NSGS mice (Figures 3A and 4E–4F). A heterozygous *TET2* mutation was the most frequent genetic alteration, and 92% of the cells carried this lesion, as evidenced by a mutational allele frequency of 46%, indicating that this is likely to be the founder clone in this patient. The other lesions, (*U2AF1* and del(*RUNX1*)) were detected in 80% and 44% of the cells, respectively (*U2AF1* mutational allele frequency = 40%; del(*RUNX1*) allele frequency = 22%). These data indicate that these two lesions are co-occurring and present in subclones that may have evolved from the founder clone in a linear fashion (Figures 4E and 4F). Subsequent analysis of $hCD45^+$ cells isolated from xenografted mice (two NSG and two NSGS) showed that del(*RUNX1*)-bearing cells were not detectable in the NSGS model (NSGS11 and NSGS12). Similarly, the *U2AF1*-bearing clone is largely outcompeted in this model by the founder *TET2*-only-bearing clone. In contrast NSG mice display engraftment of all three clones detected in the original patient bone marrow, albeit at different frequencies (Figures 4E and 4F). Altogether, these data show that we observe simultaneous engraftment of independent clones in the mouse when more than one clone is present in the patient, therefore closely mimicking the patient situation (NSG9 and NSG10).

MDS Patient-Derived MSCs Differ from Healthy MSCs at the Functional Level

The data in Figure 1B demonstrate that coinjection of MDS MSCs enhances the engraftment of MDS HSCs in NSG mice. The in vitro expanded MSCs used in this study fulfill the criteria established by the International Society of Stem Cell Therapy in terms of surface phenotype ($CD45^-HLA\text{-}DR^-CD105^+CD73^+CD90^+CD44^+CD146^+$; Figure S3A) and were devoid of hematopoietic cells, including macrophages, as demonstrated by the lack of CD45 and CD14 expression as well as the undetectable expression of myeloid specific genes such as cathepsin G (*CTSG*), proteinase 3 (*PRTN3*), and matrix metallopeptidase 9 (*MMP9*) in our RNA sequencing data (Figure S3B and data not shown). In addition, MSCs were functional, given that they were able to form an ectopic bone marrow niche (ossicle) when coinjected subcutaneously with hydroxyapatite tricalcium phosphate particles (HA-TCP), a resorbable bone substitute (Bianco et al., 2013) (Figure S3C). To directly test whether a specific supporting effect is exerted by MDS patient-derived MSCs, the identical patient

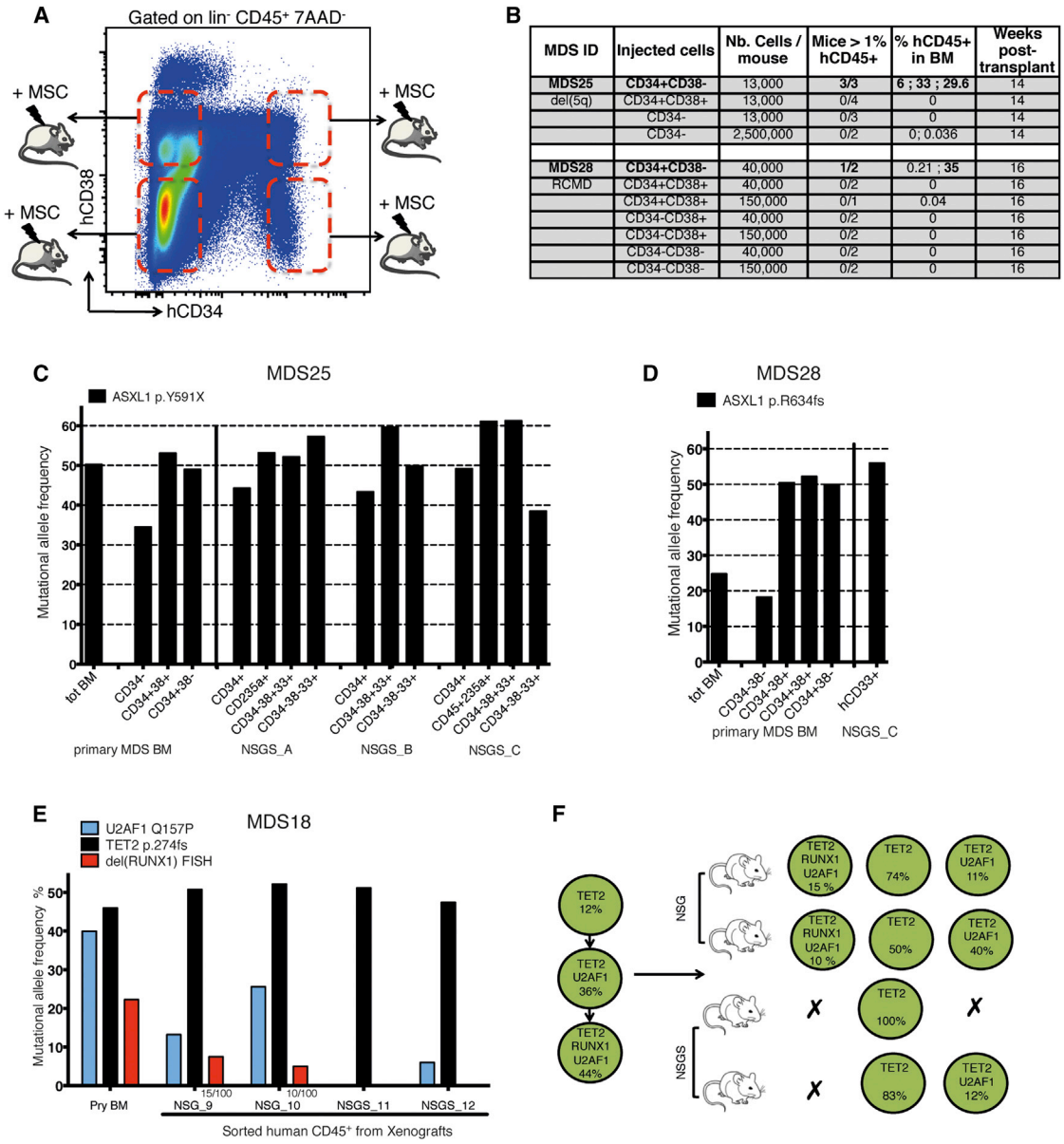

MDS ID	Injected cells	Nb. Cells / mouse	Mice > 1% hCD45+	% hCD45+ in BM	Weeks post-transplant
MDS25	**CD34+CD38-**	13,000	**3/3**	**6 ; 33 ; 29.6**	14
del(5q)	CD34+CD38+	13,000	0/4	0	14
	CD34-	13,000	0/3	0	14
	CD34-	2,500,000	0/2	0; 0.036	14
MDS28	**CD34+CD38-**	40,000	**1/2**	0.21 ; **35**	16
RCMD	CD34+CD38+	40,000	0/2	0	16
	CD34+CD38+	150,000	0/1	0.04	16
	CD34-CD38+	40,000	0/2	0	16
	CD34-CD38+	150,000	0/2	0	16
	CD34-CD38-	40,000	0/2	0	16
	CD34-CD38-	150,000	0/2	0	16

Figure 4. Disease-Propagating Stem Cells in Lower-Risk MDS Are Restricted to the Lin$^-$CD34$^+$CD38$^-$ Cell Subset and Show Variegated Clonality

(A) Gating scheme of FACS-sorted populations used for xenotransplantation into NSGS mice. Four fractions were sorted on the basis of CD34 and CD38 expression pregated on live cells (7AAD$^-$), lineage negativity (CD19, CD4, CD8, CD20, and CD235a), and positivity for CD45.

(B) Number of injected cells and engraftment results 14–16 weeks posttransplantation.

(C and D) Mutation tracking and quantification by pyrosequencing in all sorted subfractions of the primary patient as well as subpopulations of the human cells isolated from the engrafted NSGS mice.

(E and F) Detection of variegated clonality by molecular analysis of primary bone marrow cells isolated from patient MDS18 (Pry BM) and hCD45$^+$ cells from the corresponding xenografted mice. The numbers below the red bars represent the number of del(*RUNX1*)$^+$ cells scored by interphase FISH over the total number of cells analyzed. For the primary bone marrow sample, del(*RUNX1*) was evaluated by SNP array. Data show that the primary MDS patient sample is composed of three different clones containing successively accumulated mutations in the following order: *TET2*, *U2AF1*, and a genomic deletion of *RUNX1*.

See also Tables S1, S2, and S3.

sample was either cotransplanted with MDS MSCs or age-matched healthy MSCs obtained from patients undergoing hip replacement surgery. Our data show that MDS MSCs provided CD34$^+$ MDS cells with significantly enhanced engraftment capacity in all five patients tested ($p = 0.03$; Figures 5A and 5B)

MDS Patient-Derived MSCs Exhibit Specific Key Molecular Features, which Can Be Directly Induced by MDS Cells

To determine whether MDS-derived MSCs are altered, we compared their transcriptomes with age-matched healthy

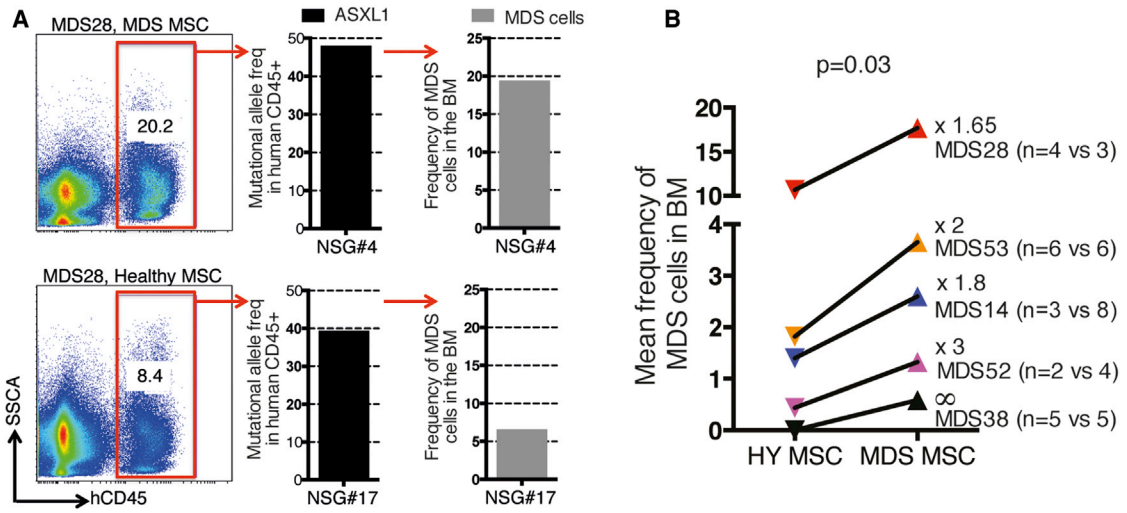

Figure 5. Comparison of MDS Engraftment with MDS MSCs as Compared to Age-Matched Healthy MSCs

(A) Exemplary FACS plots depicting differential MDS engraftment of MDS28 patient sample in NSG mice cotransplanted with either MDS MSCs or healthy MSCs derived from an age-matched donor (left) and inference of the frequency of engrafted MDS cells as determined by multiplication of the fraction of hCD45$^+$ cells carrying the MDS-specific molecular lesion (here, *ASXL1*) by the percentage of hCD45$^+$ cells in the bone marrow of engrafted mice (graphs on the right).

(B) Summary of paired analysis performed as described in (A) with five different primary patients (MDS14, MDS28, MDS38, MDS52, and MDS53). Data show a significant increase in the mean frequency of MDS cells engrafting when using MDS-derived MSCs (one-sided Wilcoxon test; p = 0.03).

See also Table S1.

MSCs (healthy MSCs, n = 3; MDS MSCs, n = 5) by RNA NGS. This analysis revealed 1,008 differentially expressed genes (q value < 0.1; 584 upregulated and 424 downregulated in MDS MSCs; Figure 6A). Gene set enrichment analysis (GSEA) (Subramanian et al., 2005) revealed that MDS MSCs exhibit a significant depletion of gene sets associated with adipogenesis with a concomitant enrichment in gene sets reflective of a mesenchymal and osteoprogenitors cell fate (Figures S4A and S4B). In addition, MDS MSCs exhibit signs of ongoing stromal stimulation and response to an inflammatory environment (Figure 6B). This is paralleled by the increased expression of genes associated with fibrosis (*LOXL2*, *SPARC*, and *ADAMTS4*), a clinical feature often observed in MDS (Figure 6C). Most importantly, our analysis also identified gene sets including cellular adhesion, extracellular matrix remodeling, and cytokine-cytokine receptor interaction to be significantly enriched in MDS MSCs (Figure 6D). These data support the view that patient MSCs might establish a specific pattern of MSC-hematopoietic MDS cell interaction within the diseased bone marrow. To validate some of these candidates, real-time RT-PCR, western blotting, and ELISA analysis were performed (Figures 6C, 6E, 6F, and S4C). Although statistical significance was achieved in the entire cohort for several factors (*VEGF-A*, *LIF*, and *ANGPTL4* and *SPARC*, *IGFBP2*, *ADAMTS4*, and *LOXL2*), others showed robust differential expression in only few patients' samples (*CCL26* and *ANG1*), reflecting an expected interpatient heterogeneity (data not shown). CDH2 (N-Cadherin), an important adhesion molecule involved in the control of HSC niche interactions and MSC-mediated protection of CML progenitors from tyrosine kinase inhibitors (Zhang et al., 2013), is also found to be highly upregulated in MDS MSCs (Figure 6E). In addition, despite being cultured in normoxic conditions, MDS MSCs maintain a strong hypoxia signature, suggesting that this program is maintained by cell-intrinsic changes at the genetic or epigenetic level (Figure S4D). Altogether, these data show that MDS MSCs have an intrinsically altered pattern of gene expression, including a number of processes involved in intercellular crosstalk, that may all contribute to their capacity to support MDS hematopoietic cells in the secondary host.

Finally, in order to test the possibility that hematopoietic MDS cells may directly induce changes in their surrounding stromal cells, we developed an in vitro coculture system in order to evaluate the effect of these cells on a healthy age-matched stroma. Healthy old MSCs were isolated from several primary donors and cocultured with either an MDS cell line, MDSL (Matsuoka et al., 2010), or primary whole bone marrow isolated from lower-risk MDS patients (Figures 7A–7C). We FACS purified the stromal cells 24 hr postincubation and evaluated the expression of *LIF* as a read out. The data show strong *LIF* induction by the exposure of healthy MSC to the MDSL (Figure 7B) or different patient-derived primary MDS bone marrow cells (Figure 7C). Importantly, exposure of the same MSCs to healthy age-matched bone marrow only marginally affected *LIF* expression (Figure 7C). These data indicate that diseased bone marrow cells are likely to play an active role in the "reprogramming" of their bone marrow niche during disease development and/or progression by possibly converting it into a self-supportive one.

Notably, in our xenotransplant model, the injected MSCs (both MDS and healthy) remained present exclusively in the injected bones for up to 4 weeks posttransplantation (Figures S5A–S5C). However, we could demonstrate engraftment of MDS-derived cells in both injected and noninjected femurs (Figure S5D). Combined with the observation that MDS hematopoietic cells can reprogram a healthy niche, these data support a model in which MDS cells further expand and migrate after the initial engraftment of the injected bone and then install disease

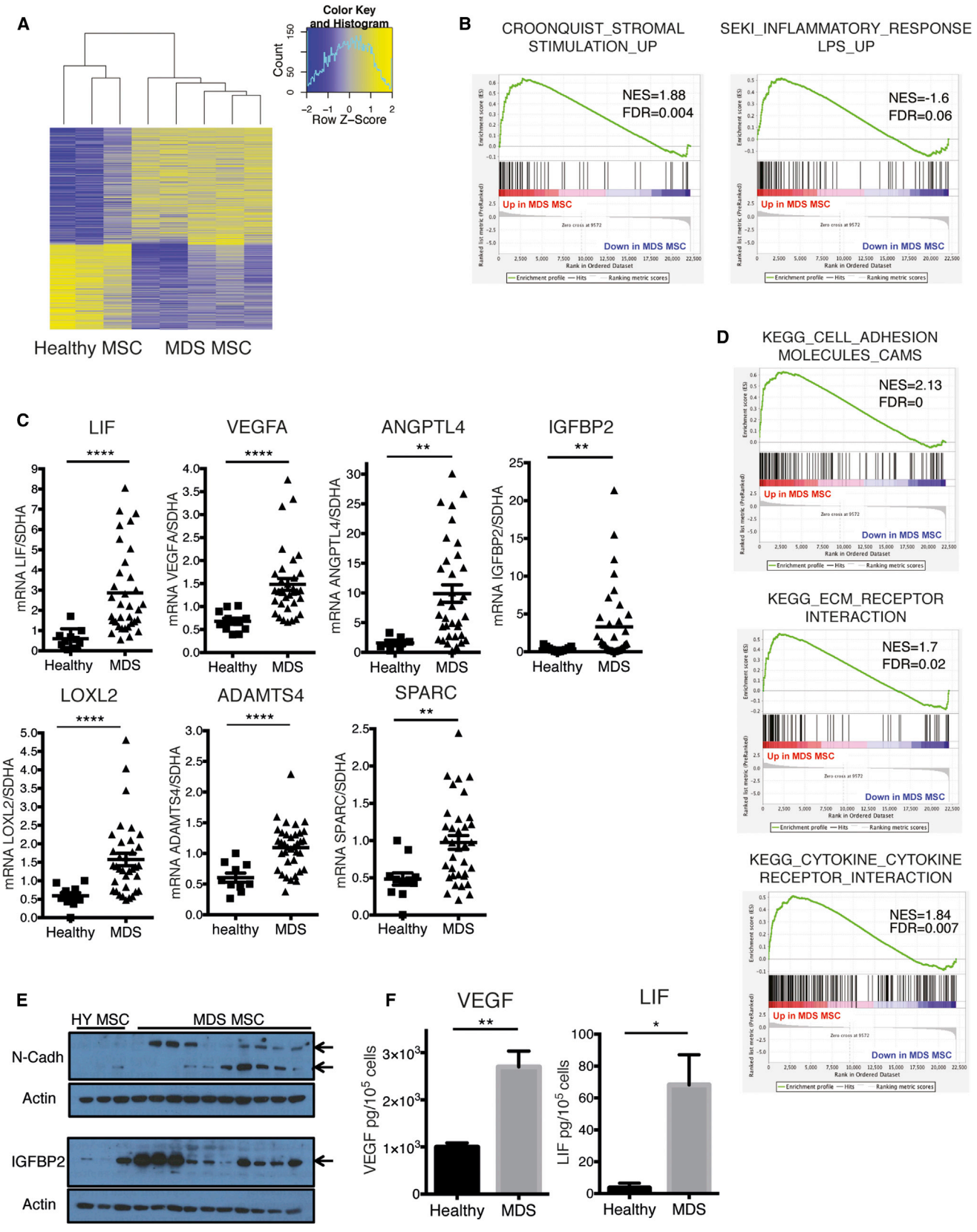

(legend on next page)

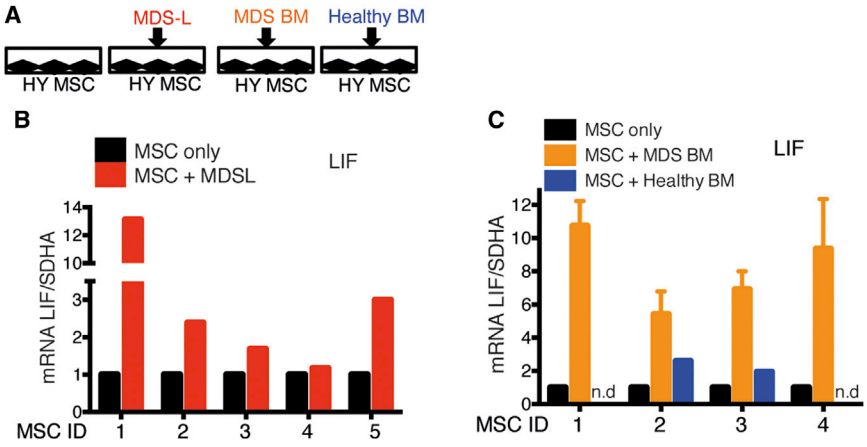

Figure 7. Exposure of Healthy MSCs to MDS Bone Marrow Leads to Altered Gene Expression

(A and B) Experimental scheme and analysis of *LIF* expression levels by qRT-PCR in five independent primary healthy old MSC cultures that were exposed to an MDS cell line (MDS-L). Data are depicted as fold change in comparison to the MSC only control culture.

(C) Analysis of *LIF* expression levels by qRT-PCR in four independent primary healthy old MSC cultures (HY MSC, black bars) that were cocultured with primary bone marrow cells derived from lower-risk MDS patients (MDS BM, orange bars). Healthy MSC culture number 1 (MSC1) was cocultured with samples MDS101 and MDS102 in two independent experiments. MSC2 was cocultured with samples MDS101, MDS102, and MDS111 in three independent experiments. MSC3 was cocultured with samples in five independent experiments (MDS101, MDS102, MDS111, MDS25, and MDS54). MSC4 was cocultured with samples MDS101 and MDS102 in two independent experiments. Statistical analysis reveals that *LIF* induction is significantly different in settings with versus without MDS cells (paired Student's t test, ****$p < 0.0001$). Healthy MSC2 and MSC3 were also exposed to healthy old (65 years old) bone marrow as a control. Data are presented as mean fold change in comparison to the corresponding MSC culture only ± SEM. All MSC cultures were depleted of any hematopoietic cells by gating out $CD45^+$ and $CD235a^+$ cells by flow cytometry before being further processed for qRT-PCR analysis (data not shown). n.d., not determined.

to the noninjected bones because of their potential to influence the mouse bone marrow stromal environment. Future studies will be necessary to explore the exact mechanism of this phenomenon.

DISCUSSION

Critically, our study identifies an intricate interplay in human MDS between mutant hematopoietic cells and their MSCs. Our data show that patient-derived hematopoietic cells instruct healthy MSCs to acquire MDS MSC-like features. In turn, MDS MSCs produce a number of cytokines and other factors to further promote the development and expansion of diseased hematopoietic MDS stem cells and their progeny. The functional relevance of this diseased "hematopoietic niche unit" for the development and progression of MDS in patients is demonstrated by its capacity to propagate MDS after orthotopic intrafemoral transplantation into NSG or NSGS mice. In contrast, the sole transplantation of $CD34^+$ MDS hematopoietic cells by our group and others only gave rise to inefficient and often transient engraftment (Martin et al., 2010; Nilsson et al., 2000; Thanopoulou et al., 2004). The use of NSGS mice, which produce human IL3, GM-CSF, and SCF (Wunderlich et al., 2010) as recipients, not only further enhanced the level of engraftment of human MDS but also retained dysplastic morphologic features typical of MDS pathology. Nevertheless, preliminary data indicate that patient MSCs remain essential for the efficient engraftment of lower-risk MDS cells even in the context of NSGS recipients, further highlighting their essential role in MDS pathogenesis (data not shown).

Importantly, beyond MDS, other myeloid neoplasms, such as CML and a subset of AMLs, have proven to be very challenging to propagate in xenografts. In addition, some studies reported that AML and MDS MSCs carry karyotype abnormalities that might hint toward functional significance for disease pathogenesis (Blau et al., 2007; Flores-Figueroa et al., 2005). Therefore, it is tempting to speculate that, similar to lower-risk MDS, CML and at least the fraction of "nonengrafter" AMLs might fail to engraft NSG mice because of a lack of a supportive environment. Niche contribution to these human myeloid neoplasms remains underappreciated, and our data point to an important area for future investigations. Consequently, this suggests that higher-risk MDS or AMLs that are transplantable by injection of $CD34^+$ cells alone have most likely acquired molecular lesions allowing them to become independent of the supporting stromal signals. Alternatively, they exhibit increased potential to rapidly reprogram the mouse stroma in order to allow disease propagation.

Figure 6. Molecular Features of MDS MSCs in Comparison to Age-Matched Healthy MSCs

(A) Heat map of 1,008 differentially regulated genes between MDS MSCs (n = 5; patients 14, 16, 17, 18, and 20; median age = 71; mean age = 68.6 ± 4) and healthy age-matched MSCs (n = 3; median age = 74; mean age = 74.4 ± 12) as determined by RNA sequencing.

(B) GSEA of RNA sequencing data showing enrichment for stromal stimulation gene sets (left) and inflammatory response (right) in MDS MSCs.

(C) Validation of differential gene expression by quantitative RT-PCR of candidate genes in a larger and independent cohort of MDS (n = 36) and age-matched healthy MSCs (n = 10; Mann-Whitney test; **$p < 0.01$; ***$p < 0.001$; ****$p < 0.0001$).

(D) GSEA showing enrichment for adhesion molecules (left), extracellular matrix and receptor genes (middle), and cytokine receptor interaction (right) in MDS MSCs.

(E) Western Blot showing differential protein expression of CDH2 (N-Cadherin) and IGFBP2 in MDS MSCs as compared to healthy MSCs.

(F) Confirmation of differential levels of VEGFA and LIF by ELISA in culture supernatants of MDS derived MSCs in comparison to age-matched healthy MSCs (Mann-Whitney test, **$p < 0.01$, *$p < 0.05$).

See also Figure S4.

To date, there are no surface markers that allow us to distinguish MDS stem cells from normal HSCs. Thus, when establishing xenograft models, it is essential to prove that the engrafted cells are indeed disease-derived as opposed to reflecting the engraftment of residual healthy HSCs present in the patients' bone marrow. The mutational tracking effort in this study demonstrates that our niche-mediated xenograft model supports the engraftment of bona fide MDS clones. In total, our approach revealed significant engraftment in 70% (14 of 20) of the patient samples transplanted with MDS MSCs. The engraftment behavior did not correlate with any clinical feature or comorbidities. Importantly, among the 14 patient samples that showed significant engraftment activity with MDS MSCs, 72% (10 of 14) showed engraftment of an MDS clone, as characterized by molecular lesion and/or a strong myeloid-biased output, whereas the remaining 28% (4 of 14) showed coengraftment of a healthy and an MDS-derived stem cell. Furthermore, the presence of stem cell ($CD34^+CD38^-$) and progenitor phenotypes ($CD34^+CD38^+$) in all xenografts 16–28 weeks posttransplantation, combined with the detection of typical MDS molecular lesions in both lymphoid and myeloid lineages in xenografts, is consistent with the engraftment of a patient derived "diseased" stem cell capable of long-term multilineage hematopoiesis. This finding argues in favor of a multipotent stem cell origin of the disease, supporting the hypotheses of others (Lawrence et al., 1987; Tehranchi et al., 2010; Thanopoulou et al., 2004; White et al., 1994). The demonstration that only $Lin^-CD34^+CD38^-$ MDS cells are able to transplant the disease further supports this conclusion and is in line with other myeloid disorders, such as CML and AML, which are believed to be initiated by mutations in normal HSCs (Corces-Zimmerman et al., 2014; Jan et al., 2012; Shlush et al., 2014; Sloma et al., 2010). This is corroborated by the results showing serial engraftment capacity, even if the MDS chimerism was relatively low in this setting. However, similar low levels of engraftment in a serial transplant setting have also been reported for aged normal HSCs (Dykstra et al., 2011), reflecting the likely reduced self-renewal capacity of aged stem cells in mouse and human.

The presence of human preleukemic HSCs, which can survive chemotherapy and provide a potential source for relapse, has recently been demonstrated by sequencing human cells in AML xenografts (Shlush et al., 2014; Corces-Zimmerman et al., 2014). In addition, whole-exome sequencing revealed that MDS bone marrow consists of distinct subclones, which are in continuous evolution during disease progression (Walter et al., 2012). The combination of our xenotransplantation workflow with quantitative mutational analyses now allows the investigation of such clonal composition and hierarchy in MDS in vivo. For example, our data imply that lower-risk MDS is driven by founder mutations such as *TET2* that initially occur in normal HSCs but then form the basis for further clonal evolution. Importantly, identification of mutations present at the stem cell level in the founder clone, as well as their specific targeting, is of relevance for the development of new treatment strategies and disease monitoring.

The identification of patient-derived MSCs as a critical functional component of lower-risk human MDS may well be relevant for other less aggressive hematological malignancies. Although it is difficult to exclude the formal possibility that a large excess of human cells might abrogate "nonspecific" causes of decreased engraftment, our data show that, in comparison to age-matched healthy MSCs, MDS MSCs significantly enhance MDS engraftment. This strongly argues in favor of the existence of a specific mechanism by which MDS MSCs support MDS $CD34^+$ engraftment in vivo. Our data are in line with recent evidence from mouse genetic studies suggesting that alterations in niche cells alone are sufficient to drive the development of myeloid malignancies in mice (Kode et al., 2014; Raaijmakers et al., 2010; Walkley et al., 2007). All of the factors differentially expressed between MDS and healthy MSCs, such as *LIF* (da Silva et al., 2005; Escary et al., 1993), *VEGFA* (Rehn et al., 2011), IGFBP2 (Garcia-Manero, 2012; Huynh et al., 2011), and *ANGPTL4* (Drake et al., 2011; Zheng et al., 2012), are known to promote survival and proliferation of both mouse and human HSPCs. Our finding that some of these factors can be induced by exposure of healthy MSCs to diseased primary MDS bone marrow cells, but not a healthy age-matched counterpart, is consistent with recent reports suggesting that leukemic cells can alter their niche counterpart in genetic mouse models of CML and AML (Schepers et al., 2013; M. Hanoun, 2013, Am. Soc. Hematol., abstract). These data support the view that a specific pattern of MSC-hematopoietic cell interaction exists within the diseased bone marrow and most likely contributes to the progressive bone marrow clonality and fibrosis frequently observed in MDS patients. Thanks to this approach, it is now possible to dissect the cellular and molecular components of this MDS niche unit in vivo, which may lead to the design of targeted strategies aimed at disrupting essential MDS MSC niche interactions. Moreover, the possibility to efficiently establish MDS xenografts from lower-risk MDS patients generates a platform for personalized oncology. Patients are still alive at the time the models are established, allowing assessment and possibly targeting of MDS pathology at the level of individual patients.

EXPERIMENTAL PROCEDURES

Detailed procedures can be found in the Supplemental Experimental Procedures.

Patient and Healthy Donor Bone Marrow Samples

MDS samples were collected from diagnostic bone marrow aspirations of MDS patients treated in the Department of Hematology and Oncology of the University Hospital Mannheim, Germany, after written informed consent. Bone marrow samples of healthy age-matched donors were obtained from residual femur specimen accrued from hip replacement surgery after written informed consent. The use of human samples was approved by the Institutional Review Board of the Medical Faculty Mannheim, University of Heidelberg, Germany, in accordance with the Declaration of Helsinki. Patient characteristics are summarized in Table S1.

Molecular Analyses

High-Density SNP Array Analyses

High-density SNP array analysis was carried out as previously reported (Nowak et al., 2012).

Screening for Commonly Mutated Genes in MDS

NGS with a screening panel for commonly mutated genes in MDS was performed as previously described (Grossmann et al., 2013; Kohlmann et al., 2011). In addition, exome sequencing was performed on an Illumina HiSeq2000 platform.

Pyrosequencing

For all mutations detected in MDS samples (single-nucleotide variations and InDels up to 4 bp), custom primer sets for validation and molecular tracking

were designed. Pyrosequencing and data analysis were performed on a Pyromark ID system (QIAGEN).

Fluorescence In Situ Hybridization

Interphase FISH was performed with the following probes: XL 5q33, D-5057-100-OG, XL AML1, and D-5027-100-OG (Metasystems), and quantitative analyses were carried out in the Munich Leukemia Laboratory.

RNA Sequencing Analysis and GSEA

RNA transcriptome sequencing was performed on a HiSeq2000 platform (Illumina). Aligned reads were converted into count tables with the htseq-count program version 0.5.4 with the gene annotation file used for read mapping. Differentially expressed genes were called with the DESeq2 package in R/Bioconductor according to the procedure outlined in the vignette. Correction for multiple testing was performed with the Benjamini-Hochberg procedure. All genes were ranked according to their log fold change and submitted to the Pre-Ranked GSEA tool and compared with 3,786 gene sets from the C2 collection of MSigDB.

Quantitative RT-PCR

RNA samples were transcribed with the SuperScript VILO cDNA synthesis kit according to the manufacturer's instructions with additional oligo-dT primers (Invitrogen). Quantitative RT-PCR was performed with the ABI Power SYBR Green Master Mix (Life Technologies). PCR reactions were performed on a Viia7 (Life Technologies) with the primers listed in Supplemental Experimental Procedures.

Flow Cytometry Analysis and Cell Sorting

FACS analysis was performed on a BD LSR Fortessa, and sorting was performed on FACSAria II and FACSAria III systems (BD Biosciences). Antibodies used are described in the Supplemental Experimental Procedures. The FACS-sorted populations used in the experiments described in Figures 3D and 3E were reanalyzed and showed over 98% purity (data not shown).

Mouse Experiments

NSG and NSGS mice were purchased from the Jackson Laboratory. Females 6–8 weeks of age were sublethally irradiated (200 cGy) before the cells were injected in the femoral bone marrow cavity. All xenotransplants were performed with 10^5 $CD34^+$ cells along with 5×10^5 MSCs unless otherwise indicated. Sample preparation is described in the Supplemental Experimental Procedures. Where indicated, fine needle aspirates from the noninjected femur were performed in order to estimate engraftment. Primary mice were analyzed 16–28 weeks posttransplanation unless indicated otherwise. For secondary transplants, FACS-sorted cells were mixed with MDS MSCs and injected according to the same procedure used for primary mice. Animals were housed under specific pathogen-free conditions at the central animal facility of the German Cancer Research Centre. All animal experiments were approved by the Animal Care Committee under Tierversuchsantrag numbers G74/12 and G210/12.

ACCESSION NUMBERS

The RNA sequencing data has been uploaded to the European Genotype Archive database for European Bioinformatics Institute and can be accessed under accession number EGAS00001000716.

SUPPLEMENTAL INFORMATION

Supplemental Information contains Supplemental Experimental Procedures, five figures and three tables and can be found with this article online at http://dx.doi.org/10.1016/j.stem.2014.02.014.

AUTHOR CONTRIBUTIONS

H.M., D.N., A.T., and W.-K.H. designed the study and wrote the manuscript. H.M. and D.N. executed most of the experiments and supervised collaborators. A.T. and W.-K.H. supervised the entire study. M.M. and J.-C.J. performed the molecular analysis and assisted with data interpretation and manuscript preparation. A.K. assisted in the establishment of the NGS analysis for molecular tracking. M.S. and C.H. performed FISH analysis. A.F. performed cytogenetic analysis. V.N., B.Z., J.O., C.K., K.M., S.F., and J.V. provided technical assistance for molecular analysis, primary MSC expansion, and mouse procedures. C.H., A.L., and C.E. assisted with RNA sequencing analysis. F.N., U.P., and N.M. contributed primary MDS patient samples. S.R., T.J., and H.R. provided healthy old bone marrow samples. E.R. and G.M. assisted with cytomorphological analysis.

ACKNOWLEDGMENTS

We thank Dr. Michael Milsom, Dr. Áine Prendergast, and David Wikström for critical comments on the manuscript. We thank Melanie Neubauer and Andrea Takacs for animal husbandry; Steffen Schmitt, Ann Atzberger, and Jens Hartwig for assistance with FACS sorting (DKFZ, Heidelberg, Germany); and Verena Haselmann and Romy Eichner (Institute of Clinical Chemistry, Mannheim, Germany) for their pyrosequencing device. A.K., M.S., and C.H. are employees of the Munich Leukemia Laboratory (MLL). The amplicon deep-sequencing assays on GS FLX and GS Junior instruments have been supported by Roche Diagnostics as part of the IRON-II study (Roche Diagnostics, Penzberg, Germany). This work was supported by the BioRN Spitzencluster Molecular and Cell-Based Medicine supported by the German Bundesministerium für Bildung und Forschung (BMBF), the SFB 873 funded by the Deutsche Forschungsgemeinschaft (DFG), the Dietmar Hopp Foundation (all A.T.), and a joint grant (IFP) of the National Center for Tumor Diseases (NCT; A.T. and D.N). H.M. was supported by a Human Frontier Science Program (HFSP) and EMBO long-term postdoctoral fellowships.

Received: May 27, 2013
Revised: December 23, 2013
Accepted: February 26, 2014
Published: April 3, 2014

REFERENCES

Abdel-Wahab, O., Gao, J., Adli, M., Dey, A., Trimarchi, T., Chung, Y.R., Kuscu, C., Hricik, T., Ndiaye-Lobry, D., Lafave, L.M., et al. (2013). Deletion of Asxl1 results in myelodysplasia and severe developmental defects in vivo. J. Exp. Med. *210*, 2641–2659.

Bejar, R., Stevenson, K., Abdel-Wahab, O., Galili, N., Nilsson, B., Garcia-Manero, G., Kantarjian, H., Raza, A., Levine, R.L., Neuberg, D., and Ebert, B.L. (2011). Clinical effect of point mutations in myelodysplastic syndromes. N. Engl. J. Med. *364*, 2496–2506.

Bejar, R., Stevenson, K.E., Caughey, B.A., Abdel-Wahab, O., Steensma, D.P., Galili, N., Raza, A., Kantarjian, H., Levine, R.L., Neuberg, D., et al. (2012). Validation of a prognostic model and the impact of mutations in patients with lower-risk myelodysplastic syndromes. J. Clin. Oncol. *30*, 3376–3382.

Bianco, P., Cao, X., Frenette, P.S., Mao, J.J., Robey, P.G., Simmons, P.J., and Wang, C.Y. (2013). The meaning, the sense and the significance: translating the science of mesenchymal stem cells into medicine. Nat. Med. *19*, 35–42.

Blau, O., Hofmann, W.K., Baldus, C.D., Thiel, G., Serbent, V., Schümann, E., Thiel, E., and Blau, I.W. (2007). Chromosomal aberrations in bone marrow mesenchymal stroma cells from patients with myelodysplastic syndrome and acute myeloblastic leukemia. Exp. Hematol. *35*, 221–229.

Corces-Zimmerman, M.R., Hong, W.J., Weissman, I.L., Medeiros, B.C., and Majeti, R. (2014). Preleukemic mutations in human acute myeloid leukemia affect epigenetic regulators and persist in remission. Proc. Natl. Acad. Sci. USA *111*, 2548–2553.

da Silva, C.L., Gonçalves, R., Crapnell, K.B., Cabral, J.M., Zanjani, E.D., and Almeida-Porada, G. (2005). A human stromal-based serum-free culture system supports the ex vivo expansion/maintenance of bone marrow and cord blood hematopoietic stem/progenitor cells. Exp. Hematol. *33*, 828–835.

Drake, A.C., Khoury, M., Leskov, I., Iliopoulou, B.P., Fragoso, M., Lodish, H., and Chen, J. (2011). Human CD34+ CD133+ hematopoietic stem cells cultured with growth factors including Angptl5 efficiently engraft adult NOD-SCID Il2rγ-/- (NSG) mice. PLoS ONE *6*, e18382.

Dykstra, B., Olthof, S., Schreuder, J., Ritsema, M., and de Haan, G. (2011). Clonal analysis reveals multiple functional defects of aged murine hematopoietic stem cells. J. Exp. Med. *208*, 2691–2703.

Escary, J.L., Perreau, J., Duménil, D., Ezine, S., and Brûlet, P. (1993). Leukaemia inhibitory factor is necessary for maintenance of haematopoietic stem cells and thymocyte stimulation. Nature *363*, 361–364.

Flores-Figueroa, E., Arana-Trejo, R.M., Gutiérrez-Espíndola, G., Pérez-Cabrera, A., and Mayani, H. (2005). Mesenchymal stem cells in myelodysplastic syndromes: phenotypic and cytogenetic characterization. Leuk. Res. *29*, 215–224.

Garcia-Manero, G. (2012). Myelodysplastic syndromes: 2012 update on diagnosis, risk-stratification, and management. Am. J. Hematol. *87*, 692–701.

Grossmann, V., Roller, A., Klein, H.U., Weissmann, S., Kern, W., Haferlach, C., Dugas, M., Haferlach, T., Schnittger, S., and Kohlmann, A. (2013). Robustness of amplicon deep sequencing underlines its utility in clinical applications. J. Mol. Diagn. *15*, 473–484.

Haferlach, T., Nagata, Y., Grossmann, V., Okuno, Y., Bacher, U., Nagae, G., Schnittger, S., Sanada, M., Kon, A., Alpermann, T., et al. (2014). Landscape of genetic lesions in 944 patients with myelodysplastic syndromes. Leukemia *28*, 241–247.

Huynh, H., Zheng, J., Umikawa, M., Zhang, C., Silvany, R., Iizuka, S., Holzenberger, M., Zhang, W., and Zhang, C.C. (2011). IGF binding protein 2 supports the survival and cycling of hematopoietic stem cells. Blood *118*, 3236–3243.

Jan, M., Snyder, T.M., Corces-Zimmerman, M.R., Vyas, P., Weissman, I.L., Quake, S.R., and Majeti, R. (2012). Clonal evolution of preleukemic hematopoietic stem cells precedes human acute myeloid leukemia. Sci. Transl. Med. *4*, ra118.

Kode, A., Manavalan, J.S., Mosialou, I., Bhagat, G., Rathinam, C.V., Luo, N., Khiabanian, H., Lee, A., Murty, V.V., Friedman, R., et al. (2014). Leukaemogenesis induced by an activating β-catenin mutation in osteoblasts. Nature *506*, 240–244.

Kohlmann, A., Klein, H.U., Weissmann, S., Bresolin, S., Chaplin, T., Cuppens, H., Haschke-Becher, E., Garicochea, B., Grossmann, V., Hanczaruk, B., et al. (2011). The Interlaboratory RObustness of Next-generation sequencing (IRON) study: a deep sequencing investigation of TET2, CBL and KRAS mutations by an international consortium involving 10 laboratories. Leukemia *25*, 1840–1848.

Lawrence, H.J., Broudy, V.C., Magenis, R.E., Olson, S., Tomar, D., Barton, S., Fitchen, J.H., and Bagby, G.C., Jr. (1987). Cytogenetic evidence for involvement of B lymphocytes in acquired idiopathic sideroblastic anemias. Blood *70*, 1003–1005.

Martin, M.G., Welch, J.S., Uy, G.L., Fehniger, T.A., Kulkarni, S., Duncavage, E.J., and Walter, M.J. (2010). Limited engraftment of low-risk myelodysplastic syndrome cells in NOD/SCID gamma-C chain knockout mice. Leukemia *24*, 1662–1664.

Matsuoka, A., Tochigi, A., Kishimoto, M., Nakahara, T., Kondo, T., Tsujioka, T., Tasaka, T., Tohyama, Y., and Tohyama, K. (2010). Lenalidomide induces cell death in an MDS-derived cell line with deletion of chromosome 5q by inhibition of cytokinesis. Leukemia *24*, 748–755.

Miller, P.H., Cheung, A.M., Beer, P.A., Knapp, D.J., Dhillon, K., Rabu, G., Rostamirad, S., Humphries, R.K., and Eaves, C.J. (2013). Enhanced normal short-term human myelopoiesis in mice engineered to express human-specific myeloid growth factors. Blood *121*, e1–e4.

Muguruma, Y., Matsushita, H., Yahata, T., Yumino, S., Tanaka, Y., Miyachi, H., Ogawa, Y., Kawada, H., Ito, M., and Ando, K. (2011). Establishment of a xenograft model of human myelodysplastic syndromes. Haematologica *96*, 543–551.

Muto, T., Sashida, G., Oshima, M., Wendt, G.R., Mochizuki-Kashio, M., Nagata, Y., Sanada, M., Miyagi, S., Saraya, A., Kamio, A., et al. (2013). Concurrent loss of Ezh2 and Tet2 cooperates in the pathogenesis of myelodysplastic disorders. J. Exp. Med. *210*, 2627–2639.

Nilsson, L., Astrand-Grundström, I., Arvidsson, I., Jacobsson, B., Hellström-Lindberg, E., Hast, R., and Jacobsen, S.E. (2000). Isolation and characterization of hematopoietic progenitor/stem cells in 5q-deleted myelodysplastic syndromes: evidence for involvement at the hematopoietic stem cell level. Blood *96*, 2012–2021.

Nowak, D., Klaumuenzer, M., Hanfstein, B., Mossner, M., Nolte, F., Nowak, V., Oblaender, J., Hecht, A., Hütter, G., Ogawa, S., et al. (2012). SNP array analysis of acute promyelocytic leukemia may be of prognostic relevance and identifies a potential high risk group with recurrent deletions on chromosomal subband 1q31.3. Genes Chromosomes Cancer *51*, 756–767.

Pang, W.W., Pluvinage, J.V., Price, E.A., Sridhar, K., Arber, D.A., Greenberg, P.L., Schrier, S.L., Park, C.Y., and Weissman, I.L. (2013). Hematopoietic stem cell and progenitor cell mechanisms in myelodysplastic syndromes. Proc. Natl. Acad. Sci. USA *110*, 3011–3016.

Papaemmanuil, E., Gerstung, M., Malcovati, L., Tauro, S., Gundem, G., Van Loo, P., Yoon, C.J., Ellis, P., Wedge, D.C., Pellagatti, A., et al.; Chronic Myeloid Disorders Working Group of the International Cancer Genome Consortium (2013). Clinical and biological implications of driver mutations in myelodysplastic syndromes. Blood *122*, 3616–3627, quiz 3699.

Raaijmakers, M.H. (2012). Myelodysplastic syndromes: revisiting the role of the bone marrow microenvironment in disease pathogenesis. Int. J. Hematol. *95*, 17–25.

Raaijmakers, M.H., Mukherjee, S., Guo, S., Zhang, S., Kobayashi, T., Schoonmaker, J.A., Ebert, B.L., Al-Shahrour, F., Hasserjian, R.P., Scadden, E.O., et al. (2010). Bone progenitor dysfunction induces myelodysplasia and secondary leukaemia. Nature *464*, 852–857.

Rehn, M., Olsson, A., Reckzeh, K., Diffner, E., Carmeliet, P., Landberg, G., and Cammenga, J. (2011). Hypoxic induction of vascular endothelial growth factor regulates murine hematopoietic stem cell function in the low-oxygenic niche. Blood *118*, 1534–1543.

Schepers, K., Pietras, E.M., Reynaud, D., Flach, J., Binnewies, M., Garg, T., Wagers, A.J., Hsiao, E.C., and Passegué, E. (2013). Myeloproliferative neoplasia remodels the endosteal bone marrow niche into a self-reinforcing leukemic niche. Cell Stem Cell *13*, 285–299.

Shlush, L.I., Zandi, S., Mitchell, A., Chen, W.C., Brandwein, J.M., Gupta, V., Kennedy, J.A., Schimmer, A.D., Schuh, A.C., Yee, K.W., et al.; HALT Pan-Leukemia Gene Panel Consortium (2014). Identification of pre-leukaemic haematopoietic stem cells in acute leukaemia. Nature *506*, 328–333.

Sloma, I., Jiang, X., Eaves, A.C., and Eaves, C.J. (2010). Insights into the stem cells of chronic myeloid leukemia. Leukemia *24*, 1823–1833.

Subramanian, A., Tamayo, P., Mootha, V.K., Mukherjee, S., Ebert, B.L., Gillette, M.A., Paulovich, A., Pomeroy, S.L., Golub, T.R., Lander, E.S., and Mesirov, J.P. (2005). Gene set enrichment analysis: a knowledge-based approach for interpreting genome-wide expression profiles. Proc. Natl. Acad. Sci. USA *102*, 15545–15550.

Tehranchi, R., Woll, P.S., Anderson, K., Buza-Vidas, N., Mizukami, T., Mead, A.J., Astrand-Grundström, I., Strömbeck, B., Horvat, A., Ferry, H., et al. (2010). Persistent malignant stem cells in del(5q) myelodysplasia in remission. N. Engl. J. Med. *363*, 1025–1037.

Thanopoulou, E., Cashman, J., Kakagianne, T., Eaves, A., Zoumbos, N., and Eaves, C. (2004). Engraftment of NOD/SCID-beta2 microglobulin null mice with multilineage neoplastic cells from patients with myelodysplastic syndrome. Blood *103*, 4285–4293.

Walenda, T., Bokermann, G., Ventura Ferreira, M.S., Piroth, D.M., Hieronymus, T., Neuss, S., Zenke, M., Ho, A.D., Müller, A.M., and Wagner, W. (2011). Synergistic effects of growth factors and mesenchymal stromal cells for expansion of hematopoietic stem and progenitor cells. Exp. Hematol. *39*, 617–628.

Walkley, C.R., Olsen, G.H., Dworkin, S., Fabb, S.A., Swann, J., McArthur, G.A., Westmoreland, S.V., Chambon, P., Scadden, D.T., and Purton, L.E. (2007). A microenvironment-induced myeloproliferative syndrome caused by retinoic acid receptor gamma deficiency. Cell *129*, 1097–1110.

Walter, M.J., Shen, D., Ding, L., Shao, J., Koboldt, D.C., Chen, K., Larson, D.E., McLellan, M.D., Dooling, D., Abbott, R., et al. (2012). Clonal architecture of secondary acute myeloid leukemia. N. Engl. J. Med. *366*, 1090–1098.

White, N.J., Nacheva, E., Asimakopoulos, F.A., Bloxham, D., Paul, B., and Green, A.R. (1994). Deletion of chromosome 20q in myelodysplasia can occur in a multipotent precursor of both myeloid cells and B cells. Blood *83*, 2809–2816.

Wunderlich, M., Chou, F.S., Link, K.A., Mizukawa, B., Perry, R.L., Carroll, M., and Mulloy, J.C. (2010). AML xenograft efficiency is significantly improved in NOD/SCID-IL2RG mice constitutively expressing human SCF, GM-CSF and IL-3. Leukemia *24*, 1785–1788.

Zhang, B., Li, M., McDonald, T., Holyoake, T.L., Moon, R.T., Campana, D., Shultz, L., and Bhatia, R. (2013). Microenvironmental protection of CML stem and progenitor cells from tyrosine kinase inhibitors through N-cadherin and Wnt-β-catenin signaling. Blood *121*, 1824–1838.

Zheng, J., Umikawa, M., Cui, C., Li, J., Chen, X., Zhang, C., Huynh, H., Kang, X., Silvany, R., Wan, X., et al. (2012). Inhibitory receptors bind ANGPTLs and support blood stem cells and leukaemia development. Nature *485*, 656–660.